

## Nb-Cr-RUTILE IN THE ORAPA KIMBERLITE, BOTSWANA

RICHARD P. TOLLO

*Department of Geology, George Washington University, Washington, D.C. 20052, U.S.A.*

STEPHEN E. HAGGERTY

*Department of Geology, University of Massachusetts, Amherst, Massachusetts 01003, U.S.A.*

### ABSTRACT

Discrete nodules (0.5 - 1 cm in diameter) of Nb-Cr-rutile, containing maximum concentrations of 20.9 wt. % Nb<sub>2</sub>O<sub>5</sub> and 8.2 wt. % Cr<sub>2</sub>O<sub>3</sub>, occur in the Orapa kimberlite in Botswana. Our data expand the compositional range of rutile from the upper mantle, and provide the first direct evidence for metasomatism at this locality. The nodules have equilibrated to coarse (1-2 mm) lamellar intergrowths of Mg-Cr-ilmenite in host Nb-Cr-rutile. The composition of this rutile, characterized by high contents of chromium and zirconium (the latter of which is strongly partitioned into this phase), differs from that of rutile in alkaline rocks, carbonatites, meteorites and lunar samples. Decomposition of armalcolite- and crichtonite-series progenitors, replacement of rutile by ilmenite, and reaction of rutile with fluids or melts are unlikely mechanisms for generating such intergrowths. Compounds of the form R<sup>2+</sup>Ti<sub>3</sub>O<sub>7</sub> would be possible precursors, but they have not been reported in high-P and high-T environments. Crystallographic shear-based structures related to α-PbO<sub>2</sub> are the most probable progenitors to accommodate the extraordinarily large concentrations of Nb, Cr, Zr and Fe at the P-T conditions of the upper mantle.

**Keywords:** kimberlite, nodules, Orapa, Botswana, rutile, ilmenite, armalcolite, crystallographic shear, mantle, metasomatism.

### SOMMAIRE

Dans la kimberlite d'Orapa, on trouve du rutile à forte teneur en Nb et Cr (jusqu'à 20.9 et 8.2% en poids de Nb<sub>2</sub>O<sub>5</sub> et Cr<sub>2</sub>O<sub>3</sub>, respectivement) sous forme de nodules de 5 à 10 mm de diamètre. Nos observations élargissent le domaine de composition du rutile du manteau supérieur et fournissent le premier témoignage de métasomatisme en cette région. Les nodules ont atteint l'équilibre en tant qu'intercroissances lamellées d'ilménite à Mg et Cr et de rutile à Nb et Cr; les lamelles d'ilménite, épaisses de 1-2 mm, sont intercalées dans celles de rutile. La composition de ce rutile, caractérisée par les teneurs élevées en Cr et Zr (ce dernier est y particulièrement concentré), diffère de celle du rutile trouvé dans les roches alcalines, carbonatites, météorites et échantillons lunaires. La décomposition de progéniteurs d'armalcolite ou de crichtonite, le remplacement du rutile par l'ilménite, la réaction du rutile avec des fluides ou des bains fondus, sont autant de mécanismes improbables pour produire pareilles intercroissances.

Les composés de la forme R<sup>2+</sup>Ti<sub>3</sub>O<sub>7</sub> pouvaient être pris en considération, mais nul composé de ce type n'a été découvert dans un environnement à hautes pression et température. Les structures cristallines à cisaillement, du type α-PbO<sub>2</sub>, seraient les précurseurs les plus probables pour affronter les hautes concentrations en Nb, Cr, Zr et Fe dans les conditions de pression et température du manteau supérieur.

(Traduit par la Rédaction)

**Mots-clés:** kimberlite, nodules, Orapa, Botswana, rutile, ilménite, armalcolite, structures à cisaillement, manteau, métasomatisme.

### INTRODUCTION

Ilmenite is a characteristic constituent of kimberlite groundmass and kimberlitic nodule suites, but rutile is uncommon in such assemblages. Rutile has been reported, however, in minor amounts from a variety of kimberlite-related associations: (1) kimberlite groundmass (Clarke & Mitchell 1975, Haggerty 1975, Elthon & Ridley 1979); (2) kimberlite autoliths (Ferguson *et al.* 1973); (3) MARID suite xenoliths in kimberlite (Dawson & Smith 1977); (4) peridotite xenoliths in kimberlite (Boullier & Nicholas 1973); (5) grosspyrite and eclogite xenoliths in kimberlite (Nixon & Boyd 1973, Sobolev 1977), and (6) inclusions in diamonds (Prinz *et al.* 1975, Meyer & Tsai 1976). The composition of rutile in such samples is characteristically close to stoichiometric TiO<sub>2</sub>, with Fe, Cr, Al and Nb present in minor concentrations only.

Intergrowths of ilmenite and rutile have been reported from a number of kimberlite localities in recent years, either as discrete nodules (Haggerty 1979, 1983, Tollo *et al.* 1981), "xenocrysts" (Shee 1979), part of the assemblage of kimberlite groundmass (Haggerty 1975, Boctor & Meyer 1979), or in association with zircon (Raber & Haggerty 1979, Haggerty & Gurney 1984). The mode of origin most commonly proposed for such ilmenite-rutile intergrowths involves the high-pressure breakdown of a precursor pseudobrookite-type phase similar to armalcolite (Fe,Mg)Ti<sub>2</sub>O<sub>5</sub> in composition (*e.g.*, Haggerty 1975, Boctor & Meyer 1979, Raber & Hag-

gerty 1979). The composition of rutile in these intergrowths, however, differs markedly from stoichiometric  $\text{TiO}_2$ ; combined  $\text{Cr}_2\text{O}_3 + \text{Nb}_2\text{O}_5$  contents may be as large as 29 wt. % (Tollo *et al.* 1981, Tollo 1982, Haggerty 1983), making armalcolite an unlikely candidate as a precursor phase. An alternative proposal is that high-pressure crystallographically sheared (CS) rutile structures are present at upper mantle P-T conditions and that these decompose upon kimberlite eruption (Haggerty 1983). Replacement of rutile by ilmenite is another possibility (Pasteris 1980).

Characterization of the petrography and mineral chemistry of ilmenite-rutile intergrowths from the Orapa kimberlite, Botswana, with new data from

Jagersfontein, expands the available data-base for these assemblages and is used to evaluate models for the genesis of such intergrowths.

#### DETERMINATIVE METHODS

Transmitted light and high-resolution oil-immersion microscopy were performed on all specimens using standard techniques. X-ray-diffraction determinations were made on duplicate subsplits of selected powdered samples using a 57.3-mm diameter camera with Ni-filtered copper  $K\alpha$  radiation ( $\lambda = 1.54050 \text{ \AA}$ ) and film mounted according to the Straumanis method.

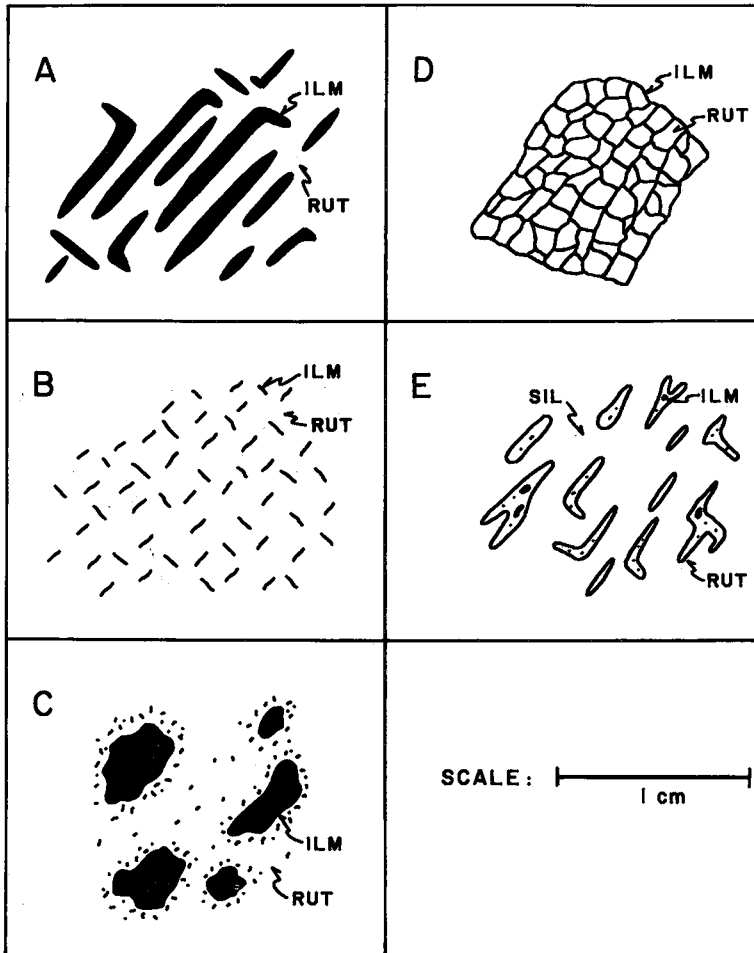


FIG. 1. Generalized classification of ilmenite-rutile intergrowth textures as viewed in polished section. (a) Coarse lamellar intergrowth with one lamellar direction dominant. (b) Fine lamellar intergrowth with individual lamellae both sigmoidal and straight in form. (c) Patchy intergrowth with fine lamellae locally concentrated around patches. (d) Polygranular atoll intergrowth consisting of ilmenite concentrated along polygranular boundaries in host rutile. (e) Symplectitic intergrowth of rutile with silicate. Note patchy and fine lamellae of ilmenite within rutile.

All electron-microbeam analyses were performed on the ETEC Autoprobe at the University of Massachusetts. Full automation of this instrument is achieved through an on-line Interdata computer using a quantitative analysis program developed jointly by the University of Massachusetts and the ETEC Corporation. Matrix corrections were employed according to the procedures of Bence & Albee (1968) and Albee & Ray (1970). Operating conditions generally included an accelerating voltage of 15 kV, an aperture current of 0.3  $\mu$ A, 15-second counting intervals for each element, and an average beam-diameter of approximately 5  $\mu$ m. Ferric iron contents were calculated for specific oxide phases using a correction procedure modified from the program FERRIC written by J. Berg & W. Kelley, which assumes: (1) perfect stoichiometry, (2) iron as the only element in multiple valence states, and (3) a perfect analysis of the other elements present. These calculations were made using the uncertainty restrictions of Finger (1972). Geochemical standards used for analysis included a variety of both natural and synthetic silicate and oxide materials from the Analytical Geochemistry Facility collection at the University of Massachusetts.

#### PETROGRAPHY

The suite consists of eleven discrete nodules recovered from the mine concentrate at the Orapa A/K-1 kimberlite pipe in Botswana and more than one dozen similar nodules collected from the Jagersfontein pipe in South Africa. The nodules from Orapa are generally black to steel-grey in color, round to ovoid in shape, with characteristically smooth surfaces, and average less than 1 cm in diameter. The nodules from Jagersfontein are generally similar in appearance, but typically smaller, averaging less than 0.5 cm in diameter. The variety of intergrowth textures observed in polished section is illustrated in Figure 1.

The coarse lamellar texture appears to be more common at Orapa than at Jagersfontein and typically consists of numerous distinct lamellae of ilmenite in regular geometric orientation within the host rutile. Ramdohr (1969, p. 987) described a similar, although presumably nonkimberlitic, intergrowth in which he considered the orientation of the lamellae to be limited to crystallographically equivalent directions within the rutile. Lamellae within the kimberlitic nodules described here are typically lens-shaped, marked by distinct reflection-anisotropy, and range from 0.5 to 2.0 mm in length and from 0.1 to 0.2 mm in width. As shown in Figure 2, ilmenite occurs in two distinct modes in these coarse lamellar intergrowths: (1) rim ilmenite situated locally along the periphery of individual nodules, or around serpentine inclusions, and (2) coherent lamel-

lae generally occupying the interior regions. The rim and lamellae ilmenite are locally continuous, with individual lamellae branching into the interior from the peripheries. Electron-microbeam analyses reveal no significant chemical differences between the two types.

The fine lamellar texture consists of numerous very fine lamellae of ilmenite oriented within the host rutile in a manner similar to that described above. Some of these samples approach the "blitz" texture described by Ramdohr (1969). These fine lamellae are typically less than 50  $\mu$ m in length and may be either straight or sigmoidal in form. Many nodules from Jagersfontein consist entirely of this texture, and several coarse lamellar nodules from both pipes show a population of very fine lamellae oriented parallel to the coarse ilmenite.

Patchy intergrowths characterize several nodules from Jagersfontein in which the ilmenite is typically oriented in an irregular pattern only locally related to obvious microfractures or possible cleavage in the host rutile. Numerous very fine lamellae of ilmenite characteristically occur in the immediate vicinity surrounding such irregular patches.

Polygranular atoll textures, on the other hand, are characterized by irregular concentrations of ilmenite along intergranular boundaries in the numerous varieties of polycrystalline rutile host. Morphologically, atoll ilmenite appears to be similar to the "external granule" texture described for ilmenite - titaniferous magnetite intergrowths by Buddington & Lindsley (1964) and may in fact also have an origin by subsolidus diffusion. The patchy ilmenite texture appears less likely to have resulted from the subsolidus diffusion of fine lamellae and may, especially where oriented along microfractures, preserve evidence of *in situ* formation of ilmenite. Areas of patchy and polygranular ilmenite coexist with fine lamellae in several polycrystalline nodules from both pipes.

Symplectitic intergrowths of rutile and silicate are relatively common in the Jagersfontein suite (Haggerty 1983, Schulze 1983), typically occurring as part of a nodule otherwise characterized by the fine lamellar, patchy, or polygranular atoll texture. Similar intergrowths are also reported from the Mbuji-Mayi kimberlite, Zaire (Ottenburgs & Fieremans 1979). The interface between coexisting silicate and rutile in such symplectites is characteristically sharp and variable in form. Very fine-scale ilmenite lamellae and patchy intergrowths occur locally within the symplectitic rutile in most specimens. The original silicate phase is typically altered beyond recognition; however, olivine and green pyroxene have been identified.

Examined in polished section, the host rutile in these nodules displays characteristic red-orange internal reflections that are typically visible along promi-

nent cleavages. Electron-microbeam (Table 1) and X-ray-diffraction (Table 2) analyses indicate that this host phase may be most appropriately classified as

*niobian rutile* according to the nomenclature of Černý *et al.* (1964). Texturally, the host rutile of these nodules varies from single, apparently

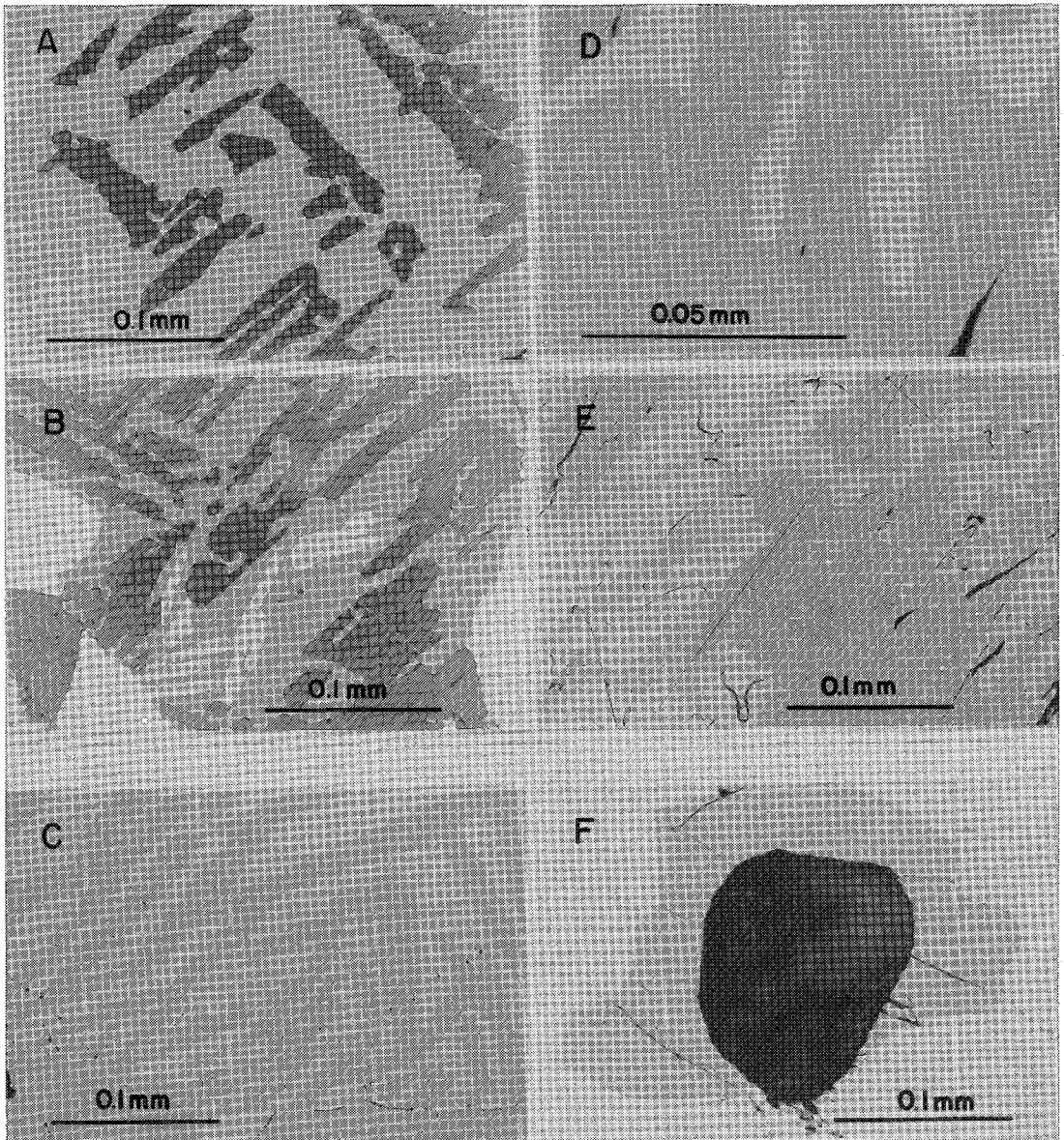


FIG. 2. Photomicrographs of ilmenite-rutile intergrowths in reflected light and under oil-immersion objectives. (a) - (b) Coarse lamellar ilmenite in orthogonal or slightly offset orthogonal angles in rutile. Variations in the color of the lamellae are due to reflection anisotropy. Granular patches of ilmenite are present at the edges of the photomicrograph in (b), with either straight or slightly sinuous contacts with the host rutile. Sample OR5-1. (c) Coarse non-orthogonal ilmenite lamellae in rutile and fine-grained ilmenite in approximately orthogonal relationship. Sample OR5-2. (d) Extremely coarse patchy ilmenite enclosing irregular blebs of host rutile. Note that the rutile has a fine set of second-generation ilmenite lamellae and that these are subparallel among rutile grains. Sample OR5-3. (e) Dominantly coarse lamellar ilmenite (white) and associated patchy ilmenite (dark grey) in rutile (light grey). This is a lower-magnification view of OR5-3 shown in (d). (f) Diffusion-controlled migration of coarse atoll ilmenite around a serpentinized (presumed olivine) inclusion in rutile. Fine lamellae of ilmenite parallel the length of the photomicrograph. Scale: width of field for (d) is 0.12 mm, and for the remainder, 0.34 mm.

TABLE 1. CHEMICAL COMPOSITIONS OF ILMENITE AND RUTILE IN ILMENITE - RUTILE INTERGROWTHS, NODULES FROM ORAPA AND JAGERSFONTEIN

Specimen:	OR-405B		OR-409B		OR-424A		OR-436A	
	rutile	ilmenite	rutile	ilmenite	rutile	ilmenite	rutile	ilmenite
TiO <sub>2</sub>	73.94	52.87	78.81	52.61	85.26	52.58	76.39	51.33
Cr <sub>2</sub> O <sub>3</sub>	7.75	3.50	6.76	4.83	5.97	2.68	7.92	3.71
Al <sub>2</sub> O <sub>3</sub>	0.03	0.00	0.08	0.09	0.04	0.01	0.02	0.00
Fe <sub>2</sub> O <sub>3</sub>	-	5.24 <sup>+</sup>	-	5.98 <sup>+</sup>	-	4.91 <sup>+</sup>	-	5.64 <sup>+</sup>
FeO	2.39 <sup>*</sup>	24.13	1.83 <sup>*</sup>	19.86	1.71 <sup>*</sup>	28.20	2.38 <sup>*</sup>	26.14
MgO	0.24	13.09	0.18	15.71	0.00	10.48	0.10	11.16
MnO	NA	0.51	NA	0.44	NA	0.48	NA	0.49
ZrO <sub>2</sub>	0.95	0.09	0.76	0.21	0.86	0.12	0.81	0.12
Nb <sub>2</sub> O <sub>5</sub>	13.38	0.57	10.46	0.86	6.94	0.24	12.73	0.52
NiO	NA	0.23	NA	0.03	NA	0.24	NA	0.26
Ta <sub>2</sub> O <sub>5</sub>	1.50	NA	1.25	NA	0.30	NA	0.42	NA
Total	100.18	100.23	100.13	100.62	101.08	99.94	100.77	99.37
Cations based on two (rutile) and three (ilmenite) oxygens								
Ti	0.796	0.913	0.836	0.890	0.881	0.927	0.811	0.906
Cr	0.088	0.064	0.076	0.086	0.065	0.049	0.088	0.069
Al	0.001	0.000	0.001	0.002	0.001	0.000	0.000	0.000
Fe <sup>3+</sup>	-	0.091	-	0.101	-	0.087	-	0.100
Fe <sup>2+</sup>	0.026	0.463	0.019	0.374	0.018	0.553	0.025	0.513
Mg	0.005	0.448	0.004	0.527	0.000	0.366	0.002	0.391
Mn	-	0.010	-	0.008	-	0.009	-	0.010
Zr	0.007	0.001	0.005	0.002	0.006	0.001	0.006	0.001
Nb	0.087	0.006	0.067	0.009	0.043	0.003	0.081	0.006
Ni	-	0.004	-	0.001	-	0.005	-	0.005
Ta	0.006	-	0.005	-	0.001	-	0.002	-
Total	1.016	2.000	1.013	2.000	1.015	2.000	1.015	2.001
n	4	9	5	4	1	4	2	4
type:	crs lamellar		fn lam/patchy		crs lamellar		crs lamellar	
modal %	66	34	-	-	79	21	75	25
NA: not analyzed      + calculated      * total iron expressed as FeO								
Specimen:	OR5-1		OR5-2		OR5-3		OR5-4	
	rutile	ilmenite	rutile	ilmenite	rutile	ilmenite	rutile	ilmenite
TiO <sub>2</sub>	64.30	49.59	70.46	52.68	73.72	53.59	73.28	52.56
Cr <sub>2</sub> O <sub>3</sub>	8.21	2.95	7.29	2.95	7.15	4.50	6.78	2.27
Al <sub>2</sub> O <sub>3</sub>	0.01	0.03	0.04	0.04	0.08	0.12	0.02	0.03
Fe <sub>2</sub> O <sub>3</sub>	-	8.00 <sup>+</sup>	-	6.06 <sup>+</sup>	-	2.68 <sup>+</sup>	-	6.93 <sup>+</sup>
FeO	4.10	25.08	2.98 <sup>*</sup>	24.10	3.17 <sup>*</sup>	24.89	3.86 <sup>*</sup>	24.13
MgO	0.41	11.64	0.64	13.41	1.12	13.28	0.43	13.21
MnO	0.05	0.49	0.01	0.50	0.05	0.51	0.03	0.54
ZrO <sub>2</sub>	1.35	0.17	1.12	0.20	1.15	0.22	1.25	0.21
Nb <sub>2</sub> O <sub>5</sub>	20.90	1.51	15.74	0.94	12.79	0.72	14.80	0.78
NiO	NA							
Ta <sub>2</sub> O <sub>5</sub>	1.54	0.00	1.21	0.03	0.84	0.00	0.04	0.00
Total	100.87	99.46	99.49	100.91	100.07	100.51	100.49	100.66
Cations based on two (rutile) and three (ilmenite) oxygens								
Ti	0.708	0.876	0.769	0.904	0.792	0.921	0.791	0.905
Cr	0.095	0.055	0.084	0.053	0.081	0.051	0.075	0.041
Al	0.000	0.001	0.001	0.001	0.001	0.003	0.000	0.010
Fe <sup>3+</sup>	-	0.141	-	0.104	-	0.046	-	0.119
Fe <sup>2+</sup>	0.050	0.493	0.036	0.460	0.038	0.476	0.036	0.462
Mg	0.009	0.407	0.014	0.456	0.024	0.453	0.010	0.451
Mn	0.001	0.010	0.000	0.010	0.001	0.010	0.001	0.001
Zr	0.010	0.002	0.008	0.002	0.008	0.002	0.009	0.002
Nb	0.138	0.016	0.103	0.010	0.083	0.007	0.094	0.008
Ni	-	-	-	-	-	-	-	-
Ta	0.001	0.000	0.005	0.000	0.003	0.000	0.002	0.000
Total	1.011	2.000	1.020	2.000	1.031	2.000	1.018	2.000
n	3	5	2	4	3	3	3	3
type:	crs lamellar		crs lamellar		crs lamellar		crs lamellar	
modal %	NA		NA		NA		NA	
Specimen:	OR5-5		OR5-6		JF-126		JF-115	
	rutile	ilmenite	rutile	ilmenite	rutile	ilmenite	rutile	ilmenite
TiO <sub>2</sub>	68.68	51.30	66.26	50.79	84.74	52.09	82.74	51.36
Cr <sub>2</sub> O <sub>3</sub>	5.06	1.52	7.78	3.07	6.77	6.84	7.13	7.00
Al <sub>2</sub> O <sub>3</sub>	0.04	0.01	0.06	0.00	0.13	0.21	0.23	0.22
Fe <sub>2</sub> O <sub>3</sub>	-	5.64 <sup>+</sup>	-	6.67 <sup>+</sup>	-	5.50 <sup>+</sup>	-	6.31 <sup>+</sup>
FeO	5.01 <sup>*</sup>	30.32	3.76 <sup>*</sup>	27.76	0.88 <sup>*</sup>	19.15	1.08 <sup>*</sup>	17.54
MgO	0.90	9.48	0.47	10.44	0.04	15.37	0.04	16.22
MnO	0.10	0.67	0.09	0.58	NA	0.26	0.00	0.32
ZrO <sub>2</sub>	1.35	0.21	1.18	0.23	0.92	0.13	1.19	0.36
Nb <sub>2</sub> O <sub>5</sub>	19.11	1.53	18.28	1.08	6.54	0.12	6.82	0.44
NiO	NA	NA	NA	NA	NA	0.24	0.10	0.19
Ta <sub>2</sub> O <sub>5</sub>	0.68	0.00	1.82	0.00	0.13	NA	0.73	0.15
Total	100.93	100.68	99.70	100.63	100.15	99.91	100.06	100.11
Cations based on two (rutile) and three (ilmenite) oxygens								
Ti	0.746	0.909	0.733	0.885	0.880	0.885	0.860	0.869
Cr	0.058	0.028	0.091	0.056	0.074	0.122	0.079	0.125
Al	0.001	0.000	0.002	0.000	0.002	0.005	0.004	0.006
Fe <sup>3+</sup>	-	0.100	-	0.134	-	0.094	-	0.107
Fe <sup>2+</sup>	0.061	0.598	0.046	0.538	0.009	0.362	0.011	0.330
Mg	0.019	0.333	0.010	0.361	0.001	0.518	0.001	0.544
Mn	0.001	0.013	0.001	0.011	-	0.005	0.000	0.006
Zr	0.009	0.002	0.008	0.003	0.006	0.002	0.008	0.004
Nb	0.125	0.016	0.122	0.011	0.041	0.001	0.048	0.004
Ni	-	-	-	-	-	0.005	0.001	0.003
Ta	0.003	0.000	0.007	0.000	0.001	-	0.003	0.001
Total	1.023	2.000	1.020	2.000	1.014	1.999	1.015	1.999
n	3	6	3	2	6	5	2	3
type:	crs lamellar		crs lamellar		crs lamellar		crs lamellar	
modal %	NA		NA		68	32	NA	

TABLE 1 (CONTINUED)

Specimen:	JG80-25		JG80-31		JG80-33		JAG26-1-1	
	rutile	ilmenite	rutile	ilmenite	rutile	ilmenite	rutile	ilmenite
TiO <sub>2</sub>	86.06	52.09	92.88	56.62	86.88	52.77	78.83	55.13
Cr <sub>2</sub> O <sub>3</sub>	6.51	7.27	4.36	3.20	6.49	5.97	4.99	2.59
Al <sub>2</sub> O <sub>3</sub>	0.09	0.31	0.01	0.24	0.07	0.37	0.08	0.06
Fe <sub>2</sub> O <sub>3</sub>	-	5.54 <sup>+</sup>	-	2.83 <sup>+</sup>	-	5.61 <sup>+</sup>	-	4.66 <sup>+</sup>
FeO	0.81*	18.78	0.07*	19.39	1.01*	19.28	1.47*	20.82
MgO	0.00	15.60	0.01	17.44	0.00	15.69	0.40	15.95
MnO	NA	0.31	NA	0.38	NA	0.31	0.06	0.26
ZrO <sub>2</sub>	0.74	0.16	1.08	0.21	0.75	0.20	1.19	0.21
Nb <sub>2</sub> O <sub>5</sub>	5.49	0.24	2.02	0.05	4.79	0.21	12.06	0.00
NiO	NA	0.29	NA	0.21	NA	0.24	0.00	0.18
Ta <sub>2</sub> O <sub>5</sub>	0.23	NA	0.14	NA	0.34	NA	NA	NA
Total	99.93	100.59	100.57	100.57	100.33	100.64	99.98	99.87
Cations based on two (rutile) and three (ilmenite) oxygens								
Ti	0.892	0.879	0.942	0.942	0.897	0.889	0.839	0.934
Cr	0.071	0.129	0.046	0.056	0.071	0.106	0.056	0.046
Al	0.002	0.008	0.000	0.006	0.001	0.010	0.001	0.002
Fe <sup>3+</sup>	-	0.094	-	0.047	-	0.095	-	0.079
Fe <sup>2+</sup>	0.008	0.353	0.001	0.359	0.010	0.362	0.017	0.393
Mg	0.000	0.522	0.000	0.576	0.000	0.524	0.008	0.536
Mn	-	0.006	-	0.007	-	0.006	0.001	0.005
Zr	0.005	0.002	0.007	0.002	0.005	0.002	0.008	0.002
Nb	0.034	0.002	0.012	0.001	0.030	0.002	0.077	0.000
Ni	-	0.005	-	0.004	-	0.004	0.000	0.003
Ta	0.001	-	0.001	-	0.001	-	0.001	-
Total	1.013	2.000	1.009	2.000	1.015	2.000	1.007	2.000
n	5	5	5	5	5	6	51	49
type:	crs lamellar		patchy		crs lamellar		crs lamellar	
modal %	NA		-		NA		NA	

Specimen:	JG80-34B		JG80-44A		JG80-44C		OR-406	
	rutile	ilmenite	rutile	ilmenite	rutile	ilmenite	rutile	ilmenite
TiO <sub>2</sub>	91.56	-	91.61	-	91.03	-	84.63	-
Cr <sub>2</sub> O <sub>3</sub>	4.48	-	4.85	-	5.24	-	5.23	-
Al <sub>2</sub> O <sub>3</sub>	0.02	-	0.00	-	0.01	-	0.31	-
Fe <sub>2</sub> O <sub>3</sub>	-	-	-	-	-	-	-	-
FeO	0.07*	-	0.17*	-	0.10*	-	1.87*	-
MgO	0.00	-	0.00	-	0.00	-	0.22	-
MnO	NA	-	NA	-	NA	-	NA	-
ZrO <sub>2</sub>	1.46	-	0.99	-	1.03	-	0.93	-
Nb <sub>2</sub> O <sub>5</sub>	2.18	-	1.93	-	2.70	-	6.49	-
NiO	NA	-	NA	-	NA	-	NA	-
Ta <sub>2</sub> O <sub>5</sub>	0.02	-	0.07	-	0.01	-	0.53	-
Total	99.79	-	99.62	-	100.12	-	100.21	-
Cations based on two oxygens								
Ti	0.928	-	0.928	-	0.920	-	0.882	-
Cr	0.048	-	0.052	-	0.056	-	0.057	-
Al	0.000	-	0.000	-	0.000	-	0.005	-
Fe <sup>3+</sup>	-	-	-	-	-	-	-	-
Fe <sup>2+</sup>	0.001	-	0.002	-	0.001	-	0.019	-
Mg	0.000	-	0.000	-	0.000	-	0.004	-
Mn	-	-	-	-	-	-	-	-
Zr	0.010	-	0.006	-	0.007	-	0.006	-
Nb	0.013	-	0.012	-	0.016	-	0.041	-
Ni	-	-	-	-	-	-	-	-
Ta	0.000	-	0.000	-	0.000	-	0.002	-
Total	1.000	-	1.000	-	1.000	-	1.016	-
n	3	-	3	-	4	-	5	-
type:	poly atoll/ fn lam		poly atoll/ fn lam/ symp		poly atoll/ fn lam		homogeneous rutile	
modal %	-		-		-		-	

homogeneous crystals characteristic of the coarse lamellar intergrowths to several polycrystalline types.

A single nodule (OR-406) composed entirely of rutile has been recovered from the Orapa site. It is ovoid in shape, approximately 1 cm in elliptical diameter, and characterized by an overall smooth exterior surface and dark reddish black color. Although microbeam analyses indicate a Nb/Ta atomic ratio of approximately 20:1, detailed microscopy and X-ray-diffraction analysis have failed to delineate the presence of fine-scale Nb-rich exsolution lamellae similar to those identified by Černý *et al.* (1964) in rutile from a variety of nonkimberlitic locations worldwide.

#### MINERAL CHEMISTRY

Chemical compositions determined by electron-microbeam analysis for coexisting ilmenite and rutile from individual nodules are presented in Table 1. Only the composition of the host rutile is given for the fine lamellar intergrowths because of the probability of overlap by the microbeam during the analysis of individual fine-scale lamellae of ilmenite. The host rutile of the intergrowths shows a broad range of compositional variation and is typically characterized by significant substitution of niobium (6.5 - 20.9 wt. % Nb<sub>2</sub>O<sub>5</sub>) and chromium (5.2 - 8.2 wt. % Cr<sub>2</sub>O<sub>3</sub>). Some of the values recorded from Orapa

are the highest yet reported from kimberlites. Iron is generally present in concentrations of less than 1 wt.% FeO in rutile from Jagersfontein (Haggerty 1983), consistent with the new results in Table 1. Similar rutile from Orapa is characterized by FeO contents in the range of 1–3 wt.%. In all cases, areas for analysis were selected microscopically and are free of fine lamellae of ilmenite. Beam overlap with subsurface ilmenite is precluded by the consistency of the FeO values obtained in 3 to 5 spot analyses. Note that the total iron content is expressed in the ferrous state in Table 1, although stoichiometric charge-balance calculations suggest that a portion of the total iron may be present as  $\text{Fe}^{3+}$ . In general, evidence from electron paramagnetic resonance studies (Carter & Okaya 1960) appears to substantiate the likelihood of such substitution by ferric iron; however, the limited experimental data presently available (Webster & Bright 1961, Wittke 1967) suggest that a significant ferrous component may be present as well. The actual  $\text{Fe}^{2+}/\text{Fe}^{3+}$  ratio cannot be determined from the data presented in this study because of the possible variability in valence of some other cations present in rutile, notably niobium.

Iron contents for the combined Orapa–Jagersfontein suite define a rather limited range, with

TABLE 2. COMPARATIVE X-RAY DATA FOR RUTILE NODULE # 406 and JCPDS # 11-396

$\bar{h}k\bar{l}$	calculated d-values (Å)		
	OR-406 <sup>1</sup>	JCPDS #11-396	hkl
100	3.245	3.23	110
75	1.686	1.687	211
30	2.482	2.48	101
15	1.625	1.627	220
10	2.183	2.190	111
10	1.360	1.361	301
5	1.347	1.348	112
5	2.050	2.051	210
5	1.480	1.481	002
5	1.452	1.454	310

\* estimated visually; <sup>1</sup> d-value data reported as the mean of four individual determinations;  $\text{CuK}\alpha$  radiation ( $\lambda = 1.54050 \text{ \AA}$ ), Ni filter

values of less than 1 to 5 wt.% FeO. The  $\text{Cr}_2\text{O}_3$  contents, on the other hand, vary widely for the combined suite and show no obvious trend separating the two individual localities. Atomic ratios of Nb/Ta for rutile from both localities show strong enrichment in niobium and indicate that the host phase of these intergrowths should be classified as *niobian rutile* according to the nomenclature of Černý *et al.*

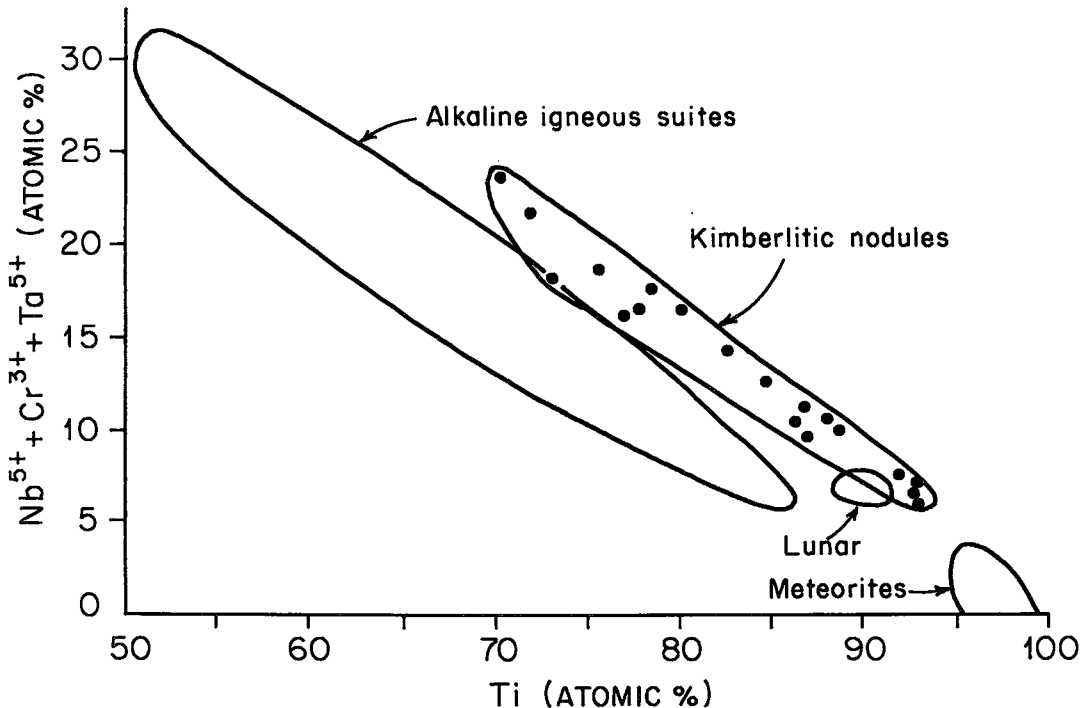


FIG. 3. Compositions of rutile from intergrowths in kimberlitic nodules (this study), lunar surface materials, meteorites and terrestrial igneous rocks plotted in terms of atomic percent Ti versus  $(\text{Nb}^{5+} + \text{Cr}^{3+} + \text{Ta}^{5+})$ . Data for the nonkimberlitic fields are taken from the literature (see text for specific references). The open circle represents Orapa nodule OR-406.

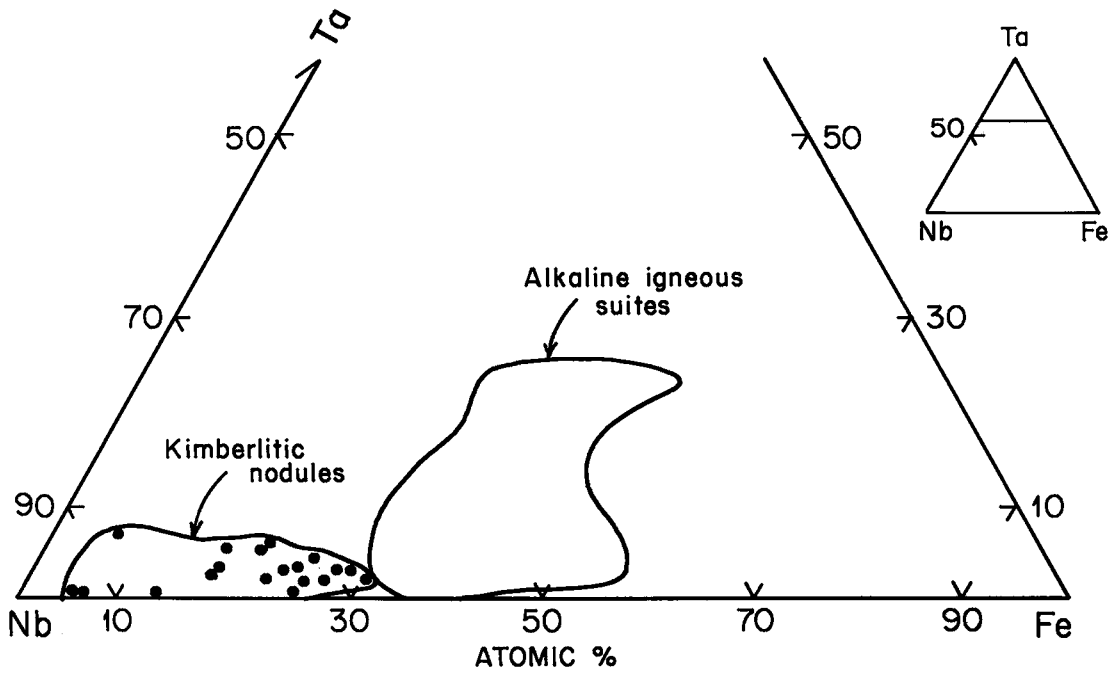


FIG. 4. Compositions of niobian rutile from kimberlitic nodules (this study) and various alkaline igneous rocks (see text for literature sources) plotted in terms of atomic percent Nb-Fe-Ta. The open circle represents Orapa nodule OR-406.

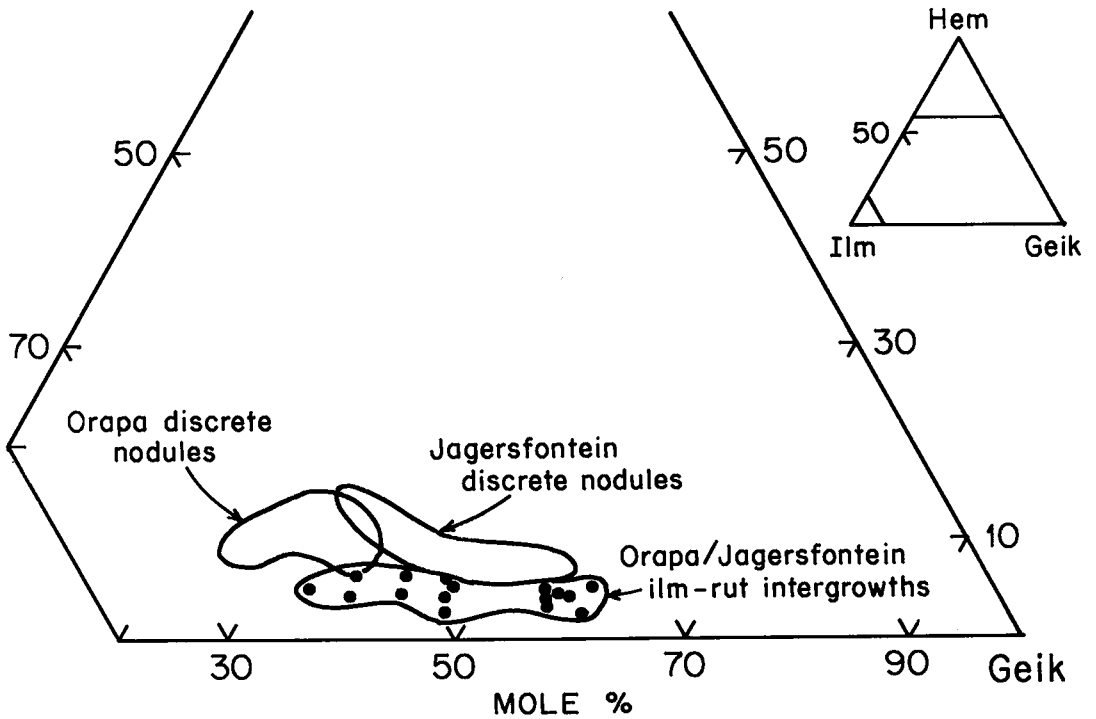


FIG. 5. Compositions of ilmenite from coarse lamellar, patchy and atoll-type intergrowths with rutile plotted in the ternary system ilmenite-geikielite-hematite. The compositions of individual discrete nodules of ilmenite from Orapa and Jagersfontein are plotted for comparison.

(1964). X-ray-diffraction analysis of a single crystal of rutile from Orapa (Table 2) supports this classification.

Rutile compositions obtained from nodules from both Orapa and Jagersfontein are plotted in Figures 3 and 4. In Figure 3, the samples of kimberlitic rutile from this study define a narrow compositional field distinct from those of similar rutile from meteorites (El Goresy 1971) and terrestrial alkaline igneous suites (Palache *et al.* 1944, Černý *et al.* 1964, Siivola 1970). The compositions of two rutile samples obtained from lunar surface materials (Marvin 1971,

Hlava *et al.* 1972) are also plotted and show an overlap with part of the kimberlitic field. It should be noted that the field of alkaline igneous rutile is in fact composed of two slightly overlapping populations: rutile from granitic pegmatites and related rocks at low  $\text{TiO}_2$  values and rutile from carbonatites and associated intrusive bodies at higher values of  $\text{TiO}_2$ . In general, rutile from granites and granitic pegmatite complexes is characterized by a lower Nb/Ta value and may be contrasted with the relatively Nb-enriched carbonatitic rutile. In Figure 4, kimberlitic rutile plots in a distinct, relatively res-

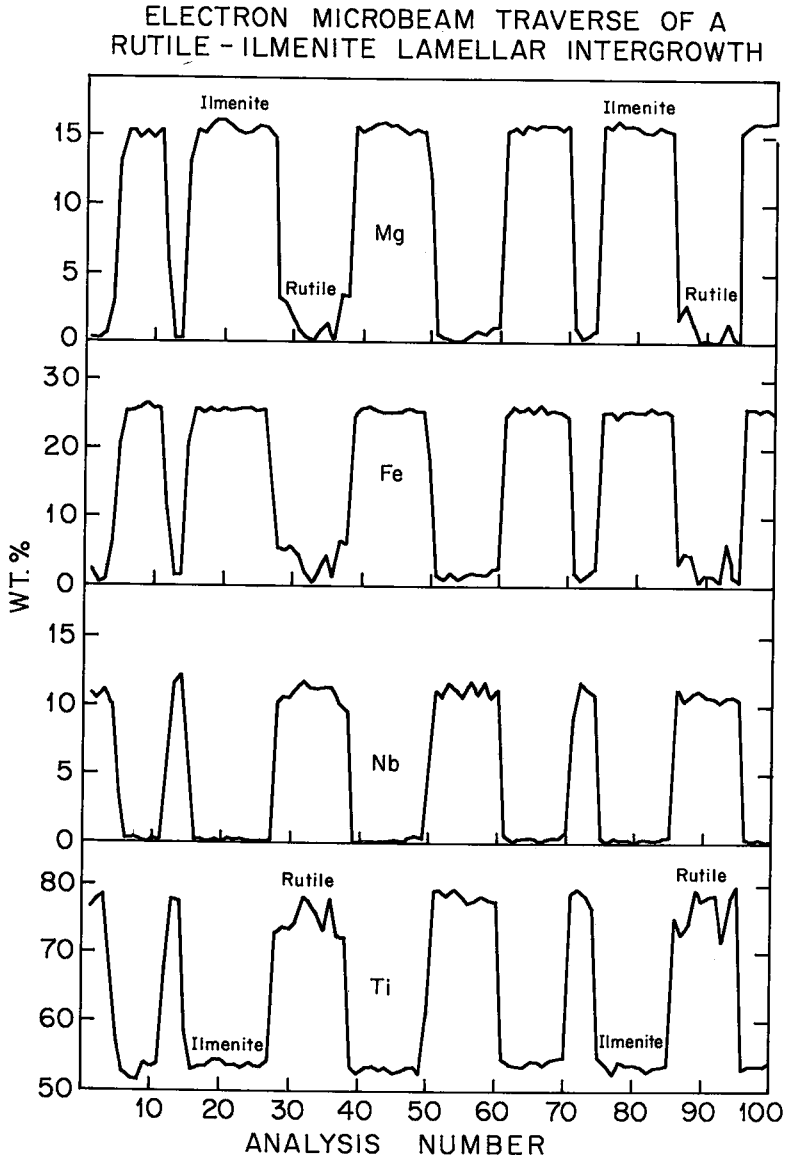


FIG. 6. Electron-microbeam traverse of an ilmenite-rutile lamellar intergrowth.

stricted field showing considerable enrichment in niobium, limited substitution of iron, and only a slight amount of tantalum. On the other hand, rutile from alkaline igneous suites appears to be characterized by a greater extent of substitution of both iron and tantalum, and by lower concentrations of niobium. Within this field, rutile from carbonatitic complexes tends to cluster closer to the Nb-Fe sideline than rutile from granitic pegmatites, which characteristically show a greater extent of Ta substitution.

Ilmenite compositions presented in Table 1 from coarse lamellar, patchy, and polygranular atoll-type intergrowths with rutile from both Orapa and Jagersfontein are clearly kimberlitic in character, with MgO and Cr<sub>2</sub>O<sub>3</sub> values ranging from 9.5 to 17.4 wt.% and from 1.5 to 7.3 wt.%, respectively. The Jagersfontein ilmenite is, on average, more magnesian and more chromian than the ilmenite from Orapa. Individual compositions, plotted in terms of the ternary solid-solution end-members FeTiO<sub>3</sub>-MgTiO<sub>3</sub>-Fe<sub>2</sub>O<sub>3</sub> in Figure 5, define a distinct linear grouping oriented nearly parallel to the ilmenite-geikielite sideline at approximately 5 mole % hematite. The main compositional fields of the ilmenite in discrete nodules from both Orapa (this study) and Jagersfontein (Haggerty, unpubl. data) are also plotted for comparison. The three fields show very little overlap, with the Jagersfontein discrete nodules typically more magnesian than their counterparts from Orapa, thereby mirroring the same relationship shown by the respective populations of lamellae. These data suggest that the ilmenite lamellae may have equilibrated under conditions of generally similar, but possibly somewhat lower, fugacities of oxygen relative to the associated discrete nodules. The compositions of lamellae at both

pipes are, in general, more chromium-rich than the associated ilmenite in discrete nodules, thereby reflecting differences in bulk composition resulting from different modes of origin. The data presented in Table 1 represent average compositions obtained from multiple analyses of several ilmenite spots within individual intergrowths. Detailed microbeam-analyses of numerous lamellae of ilmenite from individual coarse lamellar intergrowths demonstrate a typical variability of up to 2 wt.% MgO. These data, however, fail to delineate any consistent spatial patterns characterizing this inhomogeneity within individual lamellae. Data for selected elements from a detailed microbeam-traverse across such an intergrowth are presented in Figure 6, demonstrating in addition that rutile compositions may also vary, with values of FeO and TiO<sub>2</sub> typically fluctuating within a range somewhat greater than 2 wt.%. The traverse is also instructive with regard to diffusion mechanisms in that compositional contacts have a moderate slope, but M-shaped profiles are only weakly developed.

The data in Table 1 serve to illustrate the partitioning of elements observed between coexisting ilmenite and rutile in the intergrowths from Orapa and Jagersfontein. Magnesium is almost exclusively incorporated in ilmenite, reflecting the strong mutual substitution of Mg<sup>2+</sup> for Fe<sup>2+</sup> in octahedrally coordinated structural positions in the ilmenite. Chrome values indicate that Cr<sup>3+</sup> is present in significant proportions in both minerals. For the Orapa samples, chromium is consistently concentrated in the rutile, with an average relative enrichment-factor (wt.% Cr<sub>2</sub>O<sub>3</sub> in rutile/wt.% Cr<sub>2</sub>O<sub>3</sub> in ilmenite) of approximately 2.4 for the ten samples. This factor, however, is quite close to unity for the Jagersfontein

TABLE 3. CALCULATED BULK COMPOSITIONS FOR SELECTED INTERGROWTHS

Specimen:	OR-405B	OR-424A	OR-436A	JF-126	JAG26-1-1 traverse	overall average	kimberlitic armalcolite (1)
TiO <sub>2</sub>	66.78	78.40	70.12	74.29	62.86	70.49	76.92
Cr <sub>2</sub> O <sub>3</sub>	6.30	5.28	6.87	6.79	4.00	5.85	1.64
Al <sub>2</sub> O <sub>3</sub>	0.02	0.03	0.01	0.16	0.10	0.06	0.02
FeO*	11.23	8.07	9.41	8.25	16.21	10.63	13.41
MgO	4.61	2.20	2.87	4.95	9.45	4.82	7.08
MnO	0.17	0.10	0.12	0.08	0.19	0.13	0.54
ZrO <sub>2</sub>	0.66	0.72	0.64	0.67	0.61	0.66	NR
Nb <sub>2</sub> O <sub>5</sub>	9.02	5.53	9.68	4.49	4.88	6.72	NR
NiO	0.08	0.05	0.06	0.08	0.08	0.07	NR
Ta <sub>2</sub> O <sub>5</sub>	0.99	0.24	0.32	0.09	NA	0.41	NR
Total	99.86	100.62	100.10	99.85	98.38	99.84	CaO 0.06 SiO <sub>2</sub> 0.28 Total 100.61

cations based on five oxygens

Ti <sup>4+</sup>	1.924
Cr <sup>3+</sup>	0.166
Al <sup>3+</sup>	0.004
Fe <sup>2+</sup>	0.323
Mg <sup>2+</sup>	0.262
Mn <sup>2+</sup>	0.004
Zr <sup>4+</sup>	0.011
Nb <sup>5+</sup>	0.109
Ni <sup>2+</sup>	0.002
Ta <sup>5+</sup>	0.004
Total	2.809

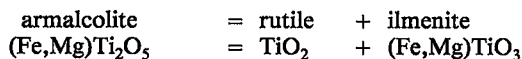
\* total iron expressed as FeO; NA; not analyzed; NR: not reported; (1) data from Haggerty (1975)

tein intergrowths. The larger cations  $Zr^{4+}$  and  $Nb^{5+}$  are clearly incorporated preferentially in the rutile from both localities, with average factors of relative enrichment of approximately 6 and 23, respectively. On the basis of similarities in ionic radii (Shannon & Prewitt 1969) and the variety of charge-balancing mechanisms of substitution possible, these patterns of element partitioning are predicted.

Bulk compositions were obtained on five coarse lamellar ilmenite-rutile intergrowths from Orapa (3) and Jagersfontein (2) by either the method of modal and compositional recombination (4 assemblages), or from the traverse average (Fig. 6) of 100 electron-microbeam analyses at 20  $\mu\text{m}$  intervals (1 assemblage). These data are presented in Table 3 along with an overall average bulk-composition. The most extreme variation is in Ti content (62.9 – 78.4 wt.%  $TiO_2$ ), followed by Mg (2.2 – 9.5 wt.% MgO). Niobium and Fe each vary by a factor of 2, but Cr (4.0 – 6.3 wt.%  $Cr_2O_3$ ) and the minor elements are more restricted.

#### GENESIS

The ilmenite-rutile intergrowths have an appearance suggestive of an origin by a subsolidus, exsolution-like process, and a range of bulk compositions indicative of armalcolite as a possible precursor phase. However, although armalcolite is relatively abundant as an early liquidus phase in certain high-titanium lunar mare basalts (e.g., Haggerty 1973), kimberlitic examples described to date occur exclusively in small amounts in the DuToitspan (Haggerty 1975), Jagersfontein (Haggerty 1983), and Bultfontein (Haggerty *et al.* 1983) kimberlites in South Africa, the Mothae kimberlite in Lesotho (Raber & Haggerty 1979), and a kimberlite in Yakutia, USSR (Tatarintsev *et al.* 1983). The close association of armalcolite with intergrowths of ilmenite and rutile at both Mothae and DuToitspan led to the suggestion that the latter phases were formed by some variant of the generalized reaction:



which is supported by experimental data (Lindsley *et al.* 1974). Rutile compositions in ilmenite-rutile intergrowths, however, differ markedly from stoichiometric  $TiO_2$ , and bulk compositions are characterized by substantial concentrations of Cr and Nb. At least four additional lines of evidence preclude armalcolite as a possible precursor: (1) kimberlitic armalcolite enriched in Cr + Nb also contains substantial calcium ( $\sim 4$  wt.% CaO), but Ca is below detection limits in the assemblages described

here; (2) armalcolite typically occurs at the interface between rutile and a silicate host and appears, therefore, to be a reaction product of  $TiO_2$  + liquid or fluid (Haggerty 1983); (3) attempts to homogenize an ilmenite-rutile intergrowth from Jagersfontein, over a range of temperatures (1000 – 1400°C) and oxygen fugacities ( $10^{-5}$  to  $10^{-13}$  atm) at 1 atm total pressure, produced armalcolite, but rutile was always an additional phase (Tollo *et al.* 1981), and (4) experimental data on the stability of armalcolite at high pressures (Lindsley *et al.* 1974, Kesson & Lindsley 1975, Friel *et al.* 1977) show that armalcolite is unstable above  $\sim 20$  kbar, the stable assemblage being rutile + ilmenite, so that a prograde reaction is required for the assemblages we describe.

Other possibilities include the decomposition of members of the crichtonite family of minerals, lindsleyite and mathiasite (Haggerty *et al.* 1983), which contain approximately 60 wt.%  $TiO_2$ . However, the large cations (Ba, K, Sr, Ca, REE), which are essential components of these phases, are not present in the ilmenite-rutile intergrowths. Replacement of rutile by ilmenite or interaction of rutile with Fe-rich fluids or melts appears unlikely because atoll textures of the type illustrated in Figure 1 are relatively rare. Bulk compositions are variable, but may be broadly modeled on  $R^{2+}Ti_3O_7$ -type compounds (Grey *et al.* 1973), satisfying high concentrations of Ti, Cr, Zr and Fe. However, the lack of confirmation regarding the substitution of Nb in the structure, the stability relations of these compounds at high pressures, and the existence of such phases in kimberlites make this possibility somewhat speculative.

Doped rutile of demonstrated high-pressure origin is structurally related to  $\alpha\text{-PbO}_2$  by crystallographic shear (Grey *et al.* 1973, Yagi *et al.* 1979, Ming *et al.* 1980). Rutile structures characterized by crystallographic shear (CS) dominate in the range of 5 – 15 wt.%  $Cr_2O_3$  (Gibb & Anderson 1972), encompassing the compositions of most rutile and the bulk compositions of ilmenite-rutile intergrowths from Orapa and Jagersfontein (Tables 1, 3). Rutile having 5 wt.% or lower  $Cr_2O_3$  contents is structurally homogeneous, and anion-deficient rutile exists with 15–17 wt.%  $Cr_2O_3$ . Niobium content in the kimberlitic intergrowths ranges from 6.5 to 20.9 wt.%  $Nb_2O_5$ , but whether or not substitution of Nb is CS-related is uncertain. Stoichiometric Nb-rutile is shown experimentally to exist at low fugacities of oxygen ( $< 10^{-12}$  atm), but nonstoichiometric compounds are present at high  $f(O_2)$  ( $> 10^{-12}$  atm) at 1000°C according to the data of Dirstine & Rosa (1979a,b). In the context of high fugacities of oxygen and nonstoichiometry, note that disordered columbite in a symplectitic intergrowth in Nb-rutile (19 – 47 wt.%  $Nb_2O_5$ ) has been described in a pegmatite (Černý *et al.* 1981). Preliminary data on one Jagersfontein ilmenite-rutile assemblage show that

CS is probably present (P. Self & P.R. Buseck, pers. comm. 1983), but in another it is absent (I. Grey, pers. comm. 1985), leaving the most likely possibility in a state of flux. The assemblages are less than ideal to evaluate the presence of CS because of extensive equilibration. Rutile grains most likely to exhibit CS are those free of "exsolved" ilmenite and containing large concentrations of Nb, Cr, Zr and Fe.

All but one of the ilmenite-rutile intergrowths are free of included or attached silicates or other oxide minerals. Serpentine, which is assumed to be derived from olivine, is the sole exception and is surrounded by ilmenite in an atoll texture (Fig. 2). Clinopyroxene, phlogopite and olivine are present in other rutile assemblages from Jagersfontein, and a metasomatic origin has been ascribed, through fluid transport and interaction with depleted harzburgite in the subcontinental lithosphere (Haggerty 1983). The fluids are enriched in titanium, alkalis and silicate-incompatible elements (Ba, Sr, Zr, Nb, REE); at Bultfontein, veinlets of K-richterite, phlogopite, diopside, lindsleyite, armalcolite and Nb-Cr-rutile develop in a harzburgitic substrate of olivine + enstatite (Jones *et al.* 1982, Haggerty *et al.* 1983). Chromium is a restite element in depleted harzburgite and is present largely in chromian spinel. Harzburgites and metasomatized harzburgites are recognized at Jagersfontein, but eclogites are the only upper-mantle nodules found at Orapa (Shee & Gurney 1979, Tollo 1982). The Nb-Cr-rutile and ilmenite assemblages, therefore, provide the first data documenting that metasomatism has also been in effect at this locality. We interpret the extreme rarity of included or attached silicate minerals to growth in coarse-grained veinlets that disaggregated upon kimberlite eruption. Phlogopite in particular is mechanically unstable, and the preservation of metasomatized nodules is generally very poor.

### CONCLUSIONS

High-pressure Nb-Cr-rutile containing lamellar ilmenite is considered to result from an exsolution-like process with strong partitioning of Nb + Zr in rutile and Mg in ilmenite, and with Cr selectively partitioned to a lesser degree in rutile. Values of Nb<sub>2</sub>O<sub>5</sub> (up to 20.9 wt. %) and Cr<sub>2</sub>O<sub>3</sub> (8.2 wt. % maximum) are higher than any previously recorded for rutile from a kimberlite. The chemically distinguishing features between kimberlitic Nb-rutile and that present in alkaline suites, pegmatites and carbonatites are high Cr and low Ta concentrations in high-pressure regimes. Meteoritic and lunar rutile is moderately enriched in Cr and overlaps with some compositions described from kimberlites.

Our data indicate that neither armalcolite- nor crichtonite-series minerals are possible precursors for

ilmenite-rutile intergrowths in kimberlites. Replacement or interaction with fluids or melts is also considered unlikely. Compounds of the form  $R^{2+}Ti_3O_7$  are possible progenitors, but these have not been identified in high-pressure associations. Equilibrated intergrowths of rutile and ilmenite are possibly related to high-pressure crystallographic-shear structures of the  $\alpha$ -PbO<sub>2</sub> type, and this is supported specifically by a correspondence in Cr contents between kimberlitic rutile and that derived experimentally.

Nb-Cr-rutile from the Orapa kimberlite is interpreted to be a product of metasomatism in coarse silicate veinlets that were disrupted because of mechanical instability. Intergrowths of the type described in this study offer potential new insights to exotic high-pressure structural forms, provide unique examples for diffusion-rate studies in the upper mantle, serve as guides to metasomatism, and represent identifiable repositories for silicate-incompatible elements.

### ACKNOWLEDGEMENTS

It is a pleasure to gratefully acknowledge the permission granted by the De Beers Mining Corporation that has enabled multiple visits to Jagersfontein and a single collecting trip to Orapa, without which this study could not have been made. The electron-microbeam facility was maintained by M.D. Leonard, and the analytical study was supported by NSF through grants EAR78-02539 and EAR83-08297 (S.E.H., principal investigator). Valuable discussions were held with J.J. Gurney, A.J. Erlank, P.R. Buseck and I. Grey, on matters relating to Orapa, metasomatism, and CS-based structures. We thank F.R. Boyd and one anonymous reviewer for helpful comments. Robin Taylor congenially performed the typing.

### REFERENCES

- ALBEE, A.L. & RAY, L. (1970): Correction factors for electron probe microanalysis of silicates, oxides, carbonates, phosphates, and sulphates. *Anal. Chem.* **42**, 1408-1414.
- BENCE, A.E. & ALBEE, A.L. (1968): Empirical correction factors for the electron microanalysis of silicates and oxides. *J. Geol.* **76**, 382-403.
- BOCTOR, N.Z. & MEYER, H.O.A. (1979): Oxide and sulfide minerals in kimberlite from Green Mountain, Colorado. In *Kimberlites, Diatremes, and Diamonds: their Geology, Petrology, and Geochemistry* (Proc. 2nd Int. Kimb. Conf., Vol. 1; F.R. Boyd & H.O.A. Meyer, eds.). Amer. Geophys. Union, Washington, D.C., 217-228.
- BOULLIER, A. & NICOLAS, A. (1973): Texture and fabric of peridotite nodules from kimberlite at Mothae,

- Thaba Putsoa and Kimberley. In Lesotho Kimberlites (P.H. Nixon, ed.). Lesotho Nat. Dev. Corp., Maseru, Lesotho.
- BUDDINGTON, A.F. & LINDSLEY, D.H. (1964): Iron-titanium oxide minerals and synthetic equivalents. *J. Petrology* **5**, 310-357.
- CARTER, D.L. & OKAYA, A. (1960): Electron paramagnetic resonance of  $\text{Fe}^{3+}$  in  $\text{TiO}_2$  (rutile). *Phys. Rev.* **118**, 1485-1490.
- ČERNÝ, P., ČECH, F. & POVONDRA, P. (1964): Review of ilmenorutile-struverite minerals. *Neues Jahrb. Mineral. Abh.* **101**, 142-172.
- \_\_\_\_\_, PAUL, B.J., HAWTHORNE, F.C. & CHAPMAN, R. (1981): A niobian rutile - disordered columbite intergrowth from the Huron Claim pegmatite, southeastern Manitoba. *Can. Mineral.* **19**, 541-548.
- CLARKE, D.B. & MITCHELL, R.H. (1975): Mineralogy and petrology of the kimberlite from Somersset Island, N.W.T., Canada. *Phys. Chem. Earth* **9**, 123-135.
- DAWSON, J.B. & SMITH, J.V. (1977): The MARID (mica-amphibole-rutile-ilmenite-diopside) suite of xenoliths in kimberlite. *Geochim. Cosmochim. Acta* **41**, 309-323.
- DIRSTINE, R.T. & ROSA, C.J. (1979a): Defect structure and related thermodynamic properties of non-stoichiometric rutile ( $\text{TiO}_{2-x}$ ) and  $\text{Nb}_2\text{O}_5$  doped rutile. I. The defect structure of  $\text{TiO}_{2-x}$  (rutile) and partial molar properties for oxygen solution at 1273 K. *Z. Metallkde* **70**, 322-329.
- \_\_\_\_\_ & \_\_\_\_\_ (1979b): Defect structure and related thermodynamic properties of nonstoichiometric rutile ( $\text{TiO}_{2-x}$ ) and  $\text{Nb}_2\text{O}_5$  doped rutile. II. The defect structure of  $\text{TiO}_2$  solid solution containing 0.1-3.0 mole %  $\text{Nb}_2\text{O}_5$  and partial molar properties for oxygen solution at 1273 K. *Z. Metallkde* **70**, 372-378.
- EL GORESY, A. (1971): Meteoritic rutile: a niobium bearing mineral. *Earth Planet. Sci. Lett.* **11**, 359-361.
- ELTHON, D. & RIDLEY, W.I. (1979): The oxide and silicate mineral chemistry of a kimberlite from the Premier mine: implications for the evolution of kimberlitic magmas. In Kimberlites, Diatremes and Diamonds: their Geology, Petrology, and Geochemistry (Proc. 2nd Int. Kimb. Conf., vol. 1; F.R. Boyd & H.O.A. Meyer, eds.), Amer. Geophys. Union, Washington, D.C., 206-216.
- FERGUSON, J., DANCHIN, R.V. & NIXON, P.H. (1973): Petrochemistry of kimberlite autoliths. In Lesotho Kimberlites (P.H. Nixon, ed.). Lesotho Nat. Dev. Corp., Maseru, Lesotho.
- ferric iron content of a microprobe analysis. *Carnegie Inst. Wash. Year Book* **71**, 600-603.
- FRIEL, J.J., HARKER, R.I. & ÜLMER, G.C. (1977): Armalcolite stability as a function of pressure and oxygen fugacity. *Geochim. Cosmochim. Acta* **41**, 403-410.
- GIBB, R.M. & ANDERSON, J.S. (1972): The system  $\text{TiO}_2$ - $\text{Cr}_2\text{O}_3$ : electron microscopy of solid solutions and crystallographic shear structures. *J. Solid State Chem.* **4**, 379-390.
- GREY, I.E., REID, A.F. & ALLPRESS, J.G. (1973): Compounds in the system  $\text{Cr}_2\text{O}_3$ - $\text{Fe}_2\text{O}_3$ - $\text{TiO}_2$ - $\text{ZrO}_2$  based on intergrowth of  $\alpha$ - $\text{PbO}_2$  and  $\text{V}_2\text{O}_5$  structural types. *J. Solid State Chem.* **8**, 86-99.
- HAGGERTY, S.E. (1973): Armalcolite and genetically associated opaque minerals in the lunar samples. *Proc. 4th Lunar Sci. Conf., Geochim. Cosmochim. Acta, Suppl.* **4**, 1, 777-797.
- \_\_\_\_\_ (1975): The chemistry and genesis of opaque minerals in kimberlites. *Phys. Chem. Earth* **9**, 295-307.
- \_\_\_\_\_ (1979): The Jagersfontein kimberlite, South Africa: an emporium of exotic mineral reactions from the upper mantle. *Kimberlite Symposium II (Cambridge)*, (abstr.).
- \_\_\_\_\_ (1983): The mineral chemistry of new titanates from the Jagersfontein kimberlite, South Africa: implications for metasomatism in the upper mantle. *Geochim. Cosmochim. Acta* **47**, 1833-1854.
- \_\_\_\_\_ & GURNEY, J.J. (1984): Zircon-bearing nodules from the upper mantle. *Trans. Amer. Geophys. Union* **65**, 305 (abstr.).
- \_\_\_\_\_, SMYTH, J.R., ERLANK, A.J., RICKARD, R.S. & DANCHIN, R.V. (1983): Lindsleyite (Ba) and mathiasite (K): two new chromium-titanates in the crichtonite series from the upper mantle. *Amer. Mineral.* **68**, 494-505.
- HLAVA, P.F., PRINZ, M. & KEIL, K. (1972): Niobian rutile in an Apollo 14 KREEP fragment. *Meteoritics* **7**, 479-485.
- JONES, A.P., SMITH, J.V. & DAWSON, J.B. (1982): Mantle metasomatism in 14 veined peridotites from Bultfontein mine, South Africa. *J. Geol.* **90**, 435-453.
- KESSON, S.E. & LINDSLEY, D.H. (1975): The effects of  $\text{Al}^{3+}$ ,  $\text{Cr}^{3+}$ , and  $\text{Ti}^{3+}$  on the stability of armalcolite. *Proc. 6th Lunar Sci. Conf., Geochim. Cosmochim. Acta, Suppl.* **6**, 1, 911-920.
- LINDSLEY, D.H., KESSON, S.E., HARTZMAN, M.J. & CUSHMAN, M.K. (1974): The stability of armalcolite: experimental studies in the system  $\text{MgO}$ - $\text{Fe}$ - $\text{Ti}$ - $\text{O}$ . *Proc. 5th Lunar Sci. Conf., Geochim. Cosmochim. Acta, Suppl.* **5**, 1, 521-534.
- FINGER, L.W. (1972): The uncertainty in the calculated

- MARVIN, U.B. (1971): Lunar niobian rutile. *Earth Planet. Sci. Lett.* **11**, 7-9.
- MEYER, H.O.A. & TSAI, H. (1976): The nature and significance of mineral inclusions in natural diamond: a review. *Mineral. Sci. Engng.* **8**, 242-261.
- MING, L.C., MANGHNANI, M.H., MATSUI, T. & JAMIESON, J.C. (1980): Phase transformations and elasticity in rutile-structured difluorides and dioxides. *Phys. Earth Planet. Int.* **23**, 276-285.
- NIXON, P.H. & BOYD, F.R. (1973): The geology of the Kao kimberlite pipes. In *Lesotho Kimberlites* (P.H. Nixon, ed.). Lesotho Nat. Dev. Corp., Maseru, Lesotho.
- OTTENBURGS, R. & FIEREMANS, M. (1979): Rutile-silicate intergrowths from the kimberlite formations at Mbuji-Mayi (Bakwanga, Zaire). *Bull. Soc. Belge Géol.* **88**, 197-203.
- PALACHE, C., BERMAN, H. & FRONDEL, C. (1944): *Dana's System of Mineralogy* (7th edition, vol. I). John Wiley & Sons, New York.
- PASTERIS, J.D. (1980): The significance of groundmass ilmenite and megacryst ilmenite in kimberlites. *Contr. Mineral. Petrology* **75**, 315-325.
- PRINZ, M., MANSON, D.V., HLAVA, P. & KEIL, K. (1975): Inclusions in diamond: garnet lherzolite and eclogite assemblages. *Phys. Chem. Earth* **9**, 797-811.
- RABER, E. & HAGGERTY, S.E. (1979): Zircon-oxide reactions in diamond-bearing kimberlites. In *Kimberlites, Diatremes, and Diamonds: their Geology, Petrology, and Geochemistry* (Proc. 2nd Int. Kimb. Conf., vol. 1; F.R. Boyd & H.O.A. Meyer, eds.). Amer. Geophys. Union, Washington, D.C., 229-240.
- RAMDOHR, P. (1969): *The Ore Minerals and Their Intergrowths*. Pergamon Press, New York.
- SCHULZE, D.J. (1983): Graphic rutile-olivine intergrowths from South African kimberlites. *Carnegie Inst. Wash. Year Book* **82**, 343-346.
- SHANNON, R.D. & PREWITT, C.T. (1969): Effective ionic radii in oxides and fluorides. *Acta Cryst.* **B25**, 925-946.
- SHEE, S.R. (1979): The opaque oxides of the Wesselton mine. *Kimberlite Symposium II (Cambridge)*, (abstr.).
- \_\_\_\_\_ & GURNEY, J.J. (1979): The mineralogy of xenoliths from Orapa, Botswana. In *The Mantle Sample: Inclusions in Kimberlites and other Volcanics* (Proc. 2nd Int. Kimb. Conf., vol. 2; F.R. Boyd & H.O.A. Meyer, eds.). Amer. Geophys. Union, Washington, D.C., 37-49.
- SHIVOLA, J. (1970): Ilmenorutile and struverite from Panikoja, Somero, SW Finland. *Bull. Geol. Soc. Finland* **42**, 33-36.
- SOBOLEV, N.V. (1977): *Deep Seated Inclusions in Kimberlites and the Problem of the Composition of the Upper Mantle* (English translation). Amer. Geophys. Union, Washington, D.C.
- TATARINTSEV, V.I., TSYMBAL, S.N., GARANIN, V.G., KUDRYATSEVA, G.P. & MARSHINTSEV, V.K. (1983): Quenched particles from kimberlites in Yakutia. *Dokl. Acad. Sci. USSR, Earth Sci. Sect.* **270**, 144-148.
- TOLLO, R.P. (1982): *Petrography and Mineral Chemistry of Ultramafic and Related Inclusions from the Orapa A/K-1 Kimberlite Pipe, Botswana*. Department of Geology and Geography Contr. **39**, Univ. Massachusetts, Amherst, Mass.
- \_\_\_\_\_, HAGGERTY, S.E. & MCMAHON, B.M. (1981): Ilmenite-rutile intergrowths in kimberlites: mineral chemistry, phase relations, and possible implications. *Trans. Amer. Geophys. Union* **62**, 414 (abstr.).
- WEBSTER, A.H. & BRIGHT, N.F.H. (1961): The system iron-titanium-oxygen at 1200°C and oxygen partial pressures between 1 Atm. and  $2 \times 10^{-14}$  Atm. *J. Amer. Ceramic Soc.* **44**, 110-116.
- WITTKÉ, J.P. (1967): Solubility of iron in TiO<sub>2</sub> (rutile). *J. Amer. Ceramic Soc.* **50**, 586-588.
- YAGI, T., JAMIESON, J.C. & MOORE, P.B. (1979): Polymorphism in MnF<sub>2</sub> (rutile type) at high pressures. *J. Geophys. Res.* **84**, 1113-1115.

Received January 13, 1986, revised manuscript accepted June 6, 1986.